

Video Article

Measurement of Maximum Isometric Force Generated by Permeabilized Skeletal Muscle Fibers

Stuart M. Roche¹, Jonathan P. Gumucio^{1,2}, Susan V. Brooks^{2,3}, Christopher L. Mendias^{1,2}, Dennis R. Clafin^{3,4}¹Department of Orthopaedic Surgery, University of Michigan Medical School²Department of Molecular & Integrative Physiology, University of Michigan Medical School³Department of Biomedical Engineering, University of Michigan Medical School⁴Department of Surgery, Section of Plastic Surgery, University of Michigan Medical SchoolCorrespondence to: Dennis R. Clafin at clafin@umich.eduURL: <http://www.jove.com/video/52695>DOI: [doi:10.3791/52695](https://doi.org/10.3791/52695)

Keywords: Bioengineering, Issue 100, Muscle physiology, skeletal muscle, single muscle fiber, permeabilized, cross-sectional area, isometric force, specific force

Date Published: 6/16/2015

Citation: Roche, S.M., Gumucio, J.P., Brooks, S.V., Mendias, C.L., Clafin, D.R. Measurement of Maximum Isometric Force Generated by Permeabilized Skeletal Muscle Fibers. *J. Vis. Exp.* (100), e52695, doi:10.3791/52695 (2015).

Abstract

Analysis of the contractile properties of chemically skinned, or permeabilized, skeletal muscle fibers offers a powerful means by which to assess muscle function at the level of the single muscle cell. Single muscle fiber studies are useful in both basic science and clinical studies. For basic studies, single muscle fiber contractility measurements allow investigation of fundamental mechanisms of force production, and analysis of muscle function in the context of genetic manipulations. Clinically, single muscle fiber studies provide useful insight into the impact of injury and disease on muscle function, and may be used to guide the understanding of muscular pathologies. In this video article we outline the steps required to prepare and isolate an individual skeletal muscle fiber segment, attach it to force-measuring apparatus, activate it to produce maximum isometric force, and estimate its cross-sectional area for the purpose of normalizing the force produced.

Video Link

The video component of this article can be found at <http://www.jove.com/video/52695/>

Introduction

The primary function of skeletal muscle is to generate force. Muscle force is elicited *in vivo* through a complex sequence of events that includes motor nerve action potentials, neuromuscular transmission, muscle fiber action potentials, release of intracellular calcium, and activation of the system of regulatory and contractile proteins. Because force generation is the ultimate result of this sequence, a deficit in force could be caused by failure of one or more of the individual steps. A key attribute of the permeabilized fiber preparation is that it eliminates most of the steps required for force generation *in vivo*, with only the regulatory and contractile functions associated with the myofibrillar apparatus remaining. The investigator assumes control over the delivery of activating calcium and energy (ATP), and is rewarded with a simplified system that allows assessment of the isolated regulatory and contractile structures in their native configuration. Measurements of force using permeabilized skeletal muscle fibers are thus valuable when assessing alterations in muscle function observed *in vivo*. For example, we have used this technique to characterize the force generating capacity of fibers from myostatin deficient mice¹ and to assess the cause of persistent muscle weakness exhibited following chronic rotator cuff tears^{2,3}.

Modern permeabilized fiber methodology can be traced to early influential studies^{4,5} and is currently in use by a number of research groups. Though the techniques have been described in the literature, they have not yet been presented in video format. The goal of this article is to illustrate an updated, valid and reliable technique for measuring the maximum force generating capacity of single fibers from chemically permeabilized skeletal muscle samples. To accomplish this, an individual fiber segment (referred to herein as a "fiber") is extracted from a pre-permeabilized bundle of fibers and placed in an experimental chamber containing a relaxing solution, the defining feature of which is a calcium concentration that is <10 nM. The fiber is then attached at one end to a force-transducer and at the other end to a length-controller. With the fiber held at an optimal sarcomere length, it is transferred to an activating solution that has a calcium concentration sufficient to elicit maximum activation and thereby maximum isometric contraction force. Force data are acquired, stored and analyzed using a personal computer.

Protocol

All procedures involving animal or human subjects should be performed in accordance with relevant guidelines, regulations, and regulatory agencies. The University of Michigan Committee on the Use and Care of Animals (UCUCA) and the University of Michigan Medical Center Institutional Review Board approved all animal and human procedures described in this article.

1. Make Dissecting and Storage Stock Solution

Note: The final volumes specified in the following instructions can be scaled up or down as desired.

- In a 1,000 ml beaker add 800 ml of deionized water (ASTM Type 1). Maintaining a gentle stir, add all the compounds listed in **Table 1** to the deionized water and allow them to dissolve.

Compound	Desired Conc. (M)	Formula Weight (g/mol)	Add to 1 L (g)
K-propionate	0.250	112.17	28.040
Imidazole	0.040	68.08	2.720
EGTA	0.010	380.40	3.800
MgCl ₂ ·6H ₂ O	0.004	203.31	0.813

Table 1: Dissecting and storage stock solution components.

- Bring to a final volume of 1,000 ml with deionized water. Note that it is unnecessary to pH the solution at this time. Store the stock solution at 4 °C.

2. Make Storage Solution

- To make 200 ml of storage solution, begin with 100 ml of dissecting and storage stock solution in a 250 ml beaker. Add sufficient Na₂H₂ATP to bring final adenosine triphosphate (ATP) concentration to 2 mM. Bring to a final volume of 200 ml with glycerol. Adjust to pH 7.00 with potassium hydroxide (KOH). Store the storage solution at -20 °C.

Note: Due to the viscous nature of glycerol it can be difficult to accurately dispense by volume. Because of this, we typically add the glycerol by weight (100 ml of glycerol weighs approximately 126 g).

3. Make Dissecting Solution

- To make 200 ml of dissecting solution, begin with 100 ml of the dissecting and storage stock solution in a 250 ml beaker.
- Add sufficient Na₂H₂ATP to bring final ATP concentration to 2 mM. Adjust pH to 7.00 with KOH. Bring the final volume to 200 ml with deionized water. Aliquot in volumes of 2.5 ml and store at -80 °C.

4. Make Dissecting Solution with Brij 58

Note: Brij 58 is a non-ionic detergent that disrupts (permeabilizes) lipid bilayers.

- To make 200 ml of dissecting solution with Brij 58, begin with 200 ml of the dissecting solution in a 250 ml beaker. Maintaining a gentle stir, add 1 g of Brij 58 (0.5% w/v) to the dissecting solution and allow it to dissolve. Aliquot in volumes of 2.5 ml and store at -80 °C.

5. Make Testing Solutions

Note: The following is adapted from Moiescu and Thieleczek 1978 (6). See Discussion for additional comments on preparing testing solutions.

- Prepare three separate 1,000 ml beakers labeled "Relaxing", "Pre-activating" and "Activating". Add 400 ml of deionized water to each beaker.
- Add the compounds indicated in **Table 2** to the appropriate beaker and then heat the solutions to between 70 °C and 80 °C. Maintain a solution temperature of 70-80 °C for 30 min while stirring continuously.

Note: A temperature of 70-80 °C assists in the elimination of carbonic acid formed by the reaction of calcium carbonate with EGTA in the activating solution. The relaxing solution and pre-activating solutions are treated in the same way as the activating solution to maintain consistency.

		RELAXING SOLUTION		PRE-ACTIVATING SOLUTION		ACTIVATING SOLUTION	
Compound	Formula Weight (g/mol)	Desired Concentration (mM)	Required Mass (g)	Desired Concentration (mM)	Required Mass (g)	Desired Concentration (mM)	Required Mass (g)
HEPES (acid)	238.30	90.0	10.724	90.0	10.724	90.00	10.724
MgO	40.31	10.3	0.208	8.5	0.171	8.12	0.164
EGTA (acid)	380.40	52.0	9.890			52.00	9.890
HDTA (acid)	348.36			50.0	8.709		
CaCO ₃	100.10					50.00	2.503

Table 2: Relaxing, pre-activating and activating solution components.

3. Cool the solution to room temperature and add sufficient NaN_3/KOH to bring the final NaN_3 concentration to 1 mM.
CAUTION: NaN_3 (sodium azide) is poisonous. Refer to the chemical MSDS prior to handling this chemical.
 1. To make 100 ml of 100 mM sodium azide solution, add 0.65 g of NaN_3 to 10 ml of 1 N KOH. Adjust to a final volume of 100 ml with deionized water.
4. Adjust the pH to approximately 7.10 using KOH.
5. Following step 5.4 add sufficient $\text{Na}_2\text{H}_2\text{ATP}$ to bring the final ATP concentration to 8 mM and sufficient Na_2CrP to bring the final creatine phosphate (CrP) concentration to 10 mM.
6. Bring each solution to the final volume of 500 ml using deionized water. Chill or heat the solutions to the temperature at which experiments will be performed, then use KOH to bring the pH to 7.10 while maintaining that temperature.
7. Add relaxing solution to the beaker containing the pre-activating solution such that the final pre-activating solution is 1 part relaxing solution in 500 pre-activating solution. Aliquot in volumes of 2.5 ml and store at -80°C .

6. Make Suture Loops

1. Begin with a strand of non-sterile USP 10-0 monofilament nylon suture.
2. Use the forceps to create a loop with the strand using the double overhand knot technique. Reduce the knot in size to approximately $750\ \mu\text{m}$ diameter. Loop diameter can be assessed under the microscope using eyepiece graticule markings.
3. Use microdissecting scissors to remove excess suture leaving only the loop and small ($500\ \mu\text{m}$) tails on either side. An example of a finished loop is shown in **Figure 1**.
4. Repeat steps 6.2-6.3 until 4 usable loops have been made. Store loops in a silicone elastomer-plated petri dish for future use.
Note: Four suture loops are required for every fiber tested.

7. Bundle Sample

Note: The following steps describe the procedure for dissecting the original sample into smaller experimental 'bundles' from which single fibers will eventually be extracted and tested. At all times the sample should be treated with care. For the purpose of this description, instructions will be given as if the investigator is right handed.

1. Obtain the sample of interest and transfer it to the facility where dissection will take place.
Note: Methods of tissue biopsy will vary depending on experimental model and study design. Where possible, muscle perfusion should be maintained up until the time of the biopsy.
2. If the sample is to be transferred between the harvest site and the dissecting site, transport it in a vial containing chilled dissecting solution while maintained on ice.
3. Prepare a 5 cm silicone elastomer-plated petri dish with chilled dissecting solution and two to three insect mounting pins ($100\ \mu\text{m}$ diameter, stainless steel).
4. Transfer the sample to the dish. Ensure that the sample remains submerged by adding more dissecting solution if necessary.
5. Inspect the sample under the microscope and manipulate it to align the longitudinal axes of the fibers toward the right shoulder of the investigator (**Figure 2**). Then anchor the sample to the dish by pinning at the corners.
Note: Make use of any remaining connective tissue as anchoring points at this time since this will maximize sample use and conserve fiber integrity. The bundle may be pinned in slight tension to assist in defining inter-fiber margins.
6. With the forceps in the left hand and the microdissecting scissors in the right, begin gently dissecting a bundle along the longitudinal margins between fibers
Note: Depending on its overall length, further dissect the bundle into numerous smaller bundles.
7. Ensure that bundle dimensions measure approximately 0.5-1 mm in width and ≥ 3 mm in length. Assess the dimensions using a microscope with graticule markings in the eyepiece, or by placing a ruler under the dish.
8. Remove and discard any tissue that is damaged by the forceps or pins as a result of the dissecting process.
9. Repeat the process until a sufficient number of bundles have been dissected or until the sample has been exhausted.
Note: The number of bundles that can be obtained will depend on numerous factors including the size and condition of the initial sample, the morphology of the muscle, and the skill of the investigator.

8. Permeabilize Fibers

1. Transfer the bundles from the dissecting solution into a vial containing 2.5 ml of fresh, chilled, dissecting solution with the non-ionic detergent 'Brij 58' added (0.5%, w/v). Incubate on ice for 30 min with occasional, gentle agitation. Ensure that the bundles remain submerged throughout incubation.
2. At the end of the 30 min incubation, transfer the bundles to a vial containing fresh dissecting solution (no Brij 58) and agitate gently and briefly to remove any remaining detergent.

9. Prepare Bundles for Storage

1. Transfer the bundles to a vial containing chilled storage solution and incubate overnight at 4°C .

10. Store Bundles

1. The following day, prepare a storage box, capable of withstanding -80°C , with enough individual 0.5 ml screw cap conical tubes to accommodate all bundles obtained during the dissecting process (one bundle per tube). Each conical tube should be filled with 200–400 μl of fresh storage solution.
2. Transfer the bundles into the individually labeled conical tubes. Ensure that the bundle is not stuck to the side of the conical tube or floating on the surface of the solution. Cap the conical tubes and store the samples at -80°C until the day of testing.

11. Prepare Experimental Apparatus

Note: The custom apparatus is composed of a stage that houses a length controller and force transducer, a moving chamber system and a 10X dissection microscope. Micrometer drive installations allow for precise manipulation of fiber attachment surfaces. Laser diffraction patterns are used to estimate sarcomere length. Data generated during experimentation is recorded on a personal computer. Refer to **Figure 3** for annotated images of the experimental set-up.

1. Thaw one vial each of the relaxing, pre-activating and activating solutions and maintain on ice. Note that ATP and CrP are labile compounds that should be maintained at cold temperatures.
2. Prepare the microscope, testing apparatus and associated computer for use.
3. Fill the first experimental chamber with relaxing solution. In our apparatus, the first chamber contains prisms that allow the investigator to photograph the fiber from the side. Fill the second experimental chamber with pre-activating solution and the third with activating solution.
4. Adjust the temperature so that the in-chamber thermometer display reads 15°C . Thread two prepared suture loops onto the stainless steel attachment surfaces extending from both the force-transducer and length-controller (**Figure 5A**).

12. Extract Permeabilized Single Fiber

1. Thaw a fiber bundle of interest, and transfer to a silicone elastomer-plated petri dish with fresh, chilled relaxing solution. Secure the bundle with pins at either end and ensure that it is submerged.
2. Using the forceps, grasp a fiber at one end and begin smoothly extracting it along its longitudinal axis.
Note: Compressive damage to the end of the fiber caused by the forceps is not a concern at this time since the contractile properties in this area will not be tested. Care should, however, be taken when extracting fibers from the bundle since adhesions between fibers and the extracellular matrix may result in excessive tension, ultimately leading to stretch-induced damage. Note that considerable variability exists among muscles in the degree to which the fibers adhere to the surrounding extracellular matrix. Fibers that are suspected to have been damaged by such a stretch should be discarded.
3. Use a razor blade or scalpel to modify a pipet tip as shown in (**Figure 4**). Introduce the fiber into the tip along with a small amount of relaxing solution. Transfer the single fiber from the silicone elastomer-plated petri dish to the experimental chamber that contains the relaxing solution.

13. Mount Single Fiber

Note: A step-by-step depiction can be viewed in **Figure 5**.

1. Guiding gently with the forceps, remove the fiber from the pipet tip and anchor it to the length-controller (left) using the first suture loop.
 1. Use a single, smooth motion when tightening the loop with the forceps. Ensure that an equal and opposite tension is applied to either end of the suture.
 2. The first loop should be tied around 1 mm to 2 mm from the end of the length-controller attachment surface.
2. Manipulate the other end of the fiber toward the force-transducer (right) and secure the fiber using the same procedure. Remove excess suture using the microdissecting scissors (**Figure 5C**).
3. Place the fiber under a small amount of tension by increasing the distance between the length-controller and force-transducer arms using the x-coordinate micrometer drive (**Figure 3A**).
4. Thread the second loop over the first and anchor the fiber at a point within 0.2 mm of the end of the force-transducer attachment surface (**Figure 5D**).
 1. Remove excess suture using the microdissecting scissors.
5. The fiber attachment process can result in loss of solution from the chamber. If necessary, add more relaxing solution to ensure the surface of the solution is flat (neither concave nor convex). A flat surface is important when assessing sarcomere length using laser diffraction.
6. Align the fiber parallel to the sidewalls of the experimental chamber by adjusting the position of the length-controller in the direction of the y-axis.
7. Survey the fiber using the prism side view and adjust the position of the length-controller in the direction of the z-axis until the fiber is parallel to the floor of the chamber.
Note: Positioning of the fiber parallel to the floor of the chamber can be accomplished without chamber prisms by focusing first on one end of the fiber and then, without adjusting the microscope focus, bringing the other end of the fiber into focus using its z-axis micrometer drive.
8. If the fiber is in any way contorted, twisted or damaged as a result of the mounting process, the fiber should be discarded and a new fiber attached.

14. Set Optimal Sarcomere Length

- When the fiber has been correctly aligned within the chamber, insert the calibrated target screen onto the anterior aspect of the microscope and align it over the first experimental chamber.
Note: The target screen is calibrated using the standard grating equation, $\lambda = SL \sin\theta$, where SL is sarcomere length, θ is the diffraction angle between the 0° and 1° diffracted beams and λ is the wavelength of the laser.
- Turn on the laser and adjust the position of the stage such that the laser passes through the center of the fiber.
CAUTION: Concentrated laser light can be damaging to eyesight. Never attempt to visualize the fiber through the microscope when the laser is on.
- Position the fiber with respect to the laser beam to diffract the laser light and observe an interference pattern on the calibrated target screen (**Figure 6**). Turn off the lights to visualize this pattern more clearly.
Note: If, with the correct positioning of the laser beam, no interference pattern is seen, this suggests that the myofibrillar components of the fiber are abnormal/damaged and that the fiber should be replaced with a fresh one.
- To set the sarcomere length, increase or decrease the tension on the fiber using the length-controller x-axis micrometer drive until the desired spacing of the diffracted light is observed on the target screen.
Note: The optimal sarcomere length of the fiber will depend on the species of animal from which the sample was obtained. A sarcomere length of $2.7 \mu\text{m}$ is commonly assumed to be optimal when assessing fibers from human tissue^{7,8}.
- After optimal sarcomere length has been set, measure the distance between the two innermost sutures. This is most easily accomplished using the digital readout on the micrometer drive that controls the x-axis motion of the chamber. Position the chamber such that the vertical cross hair of the eyepiece is aligned on the innermost border of the innermost suture and zero the digital readout on the micrometer drive.
- Translate the stage along the x-axis relative to the microscope until reaching the other innermost suture. The digital display will indicate the length of the fiber. This value should be recorded as fiber length, L_f .
Note: It should be understood that the distance between the two innermost sutures will determine the functional length of the contractile tissue being evaluated. The investigator should strive for consistency in this dimension (*i.e.* L_f) within a series of experiments.

15. Estimate Cross-sectional Area (CSA)

- Maintain the fiber at L_f and use the microscope-mounted camera to capture a high magnification image of the central portion of the fiber from both the top and side views. Side view images can be captured using the prism embedded in the side of the chamber.
Note: When shifting between top and side views it is important to move the microscope only in the y-direction to ensure that the two images are "in register" and therefore show two different views of the same section of the fiber.
- Obtain measurements at this time to normalize absolute force later in the study. The techniques for obtaining these measurements are described later and illustrated in **Figures 7A** and **7B**.

16. Elicit Isometric Contraction

Note: While data generated during these experiments may be collected and interpreted without the use of a computer, software that allows for the acquisition, display, storage and analysis of the force responses is advantageous. The custom LabVIEW software created by our laboratory allows these functions as well as the capability to design 'motion trains' that govern the action of the length-controller during an experiment.

- Confirm that the temperature of the relaxing, pre-activating and activating solutions are stable at 15°C .
- Use the chamber control software to move the fiber to the chamber containing the pre-activating solution and incubate there for 3 min.
Note: The pre-activating solution is weakly buffered for Ca^{2+} , resulting in a very rapid activation and force development upon introduction of the fiber to the activating solution.
- With 10 sec remaining in the pre-activating solution and the fiber length maintained at L_f , establish a zero force level in the experimental record.
Note: The 'Find Force Zero' movement of the length-controller reveals the force-transducer level that corresponds to zero force (*i.e.* the fiber briefly becomes slack as a result of the movement). Passive force is the difference between that zero and the force level just prior to the transducer-zeroing movement.
- At the end of the 3 min, move the fiber to the chamber containing the activating solution and allow maximum isometric force to develop as evidenced by a plateau in force that is preceded by a rapid rise.
- After reaching maximum isometric force, use the length-controller to identify the force-transducer output that corresponds to zero force in the chamber containing the activating solution.
Note: This is necessary because the force-transducer output that corresponds to zero force is, in general, different for each solution-filled chamber.
- Following attainment of a second force plateau, return the fiber to the chamber containing the relaxing solution. Testing is now complete. To test multiple fibers during any one session aspirate all solutions and add new, chilled solutions.
Note: Brenner's cycling protocols should be considered when eliciting maximal contractions over an extended period of time. This protocol has been shown to conserve structural and mechanical properties in the maximally activated fiber⁹.

Representative Results

Healthy, chemically permeabilized single fibers should appear uniform in shape and have consistent striation spacing when viewed under high magnification. Fibers that are inflexible when manipulated with the forceps or have obvious structural damage should be discarded.

High magnification digital images taken during step 15 are analyzed for 5 paired diameter measurements along the midsection of the fiber. Fiber CSA is estimated assuming an elliptical cross section and averaging 5 individual CSA measurements as depicted in **Figure 7A**. **Figure 7B** also

serves to illustrate how fiber dimensions in one view can be significantly different compared with paired dimensions in the other view (i.e., cross-sections are not, in general, round).

Representative force traces from human slow and fast fibers are shown in **Figures 8A** and **8B**, respectively. Voltage output of the force-transducer is acquired during a test and converted to force (mN) using data acquisition and analysis software (LabVIEW). **Figure 9** illustrates the approach used to assess maximum active force (F_o), which is calculated by subtracting the force required to maintain the fiber at optimal sarcomere length while in a relaxed state (passive force, F_p), from the greatest isometric force developed during maximal fiber activation (total force, F_T). Since the output of the force-transducer that corresponds to zero force is, in general, different for each of the different bathing chambers, we briefly slacken the fiber in both the pre-activating and activating solutions to capture the zero-force level in the experimental record. Normalization of maximum active force by fiber CSA is used to generate the more informative value of specific force (sF_o). Because it takes into consideration the CSA of the fiber, sF_o provides a measure of the intrinsic force generating capacity of the fiber's contractile apparatus, thereby allowing functional comparisons between fibers of disparate sizes. It should, however, be noted that CSA measurements are not able to distinguish the proportion of the fiber occupied by contractile filaments versus the proportion occupied by other subcellular structures.

Typical characteristics of healthy, adult fibers from Clafin *et al.* 2011¹⁰ for human, Mendias *et al.* 2011¹ for mouse and Gumucio *et al.* 2012² for rat are detailed in **Table 3**. All data presented in **Table 3** were generated using the techniques described in this article.

	Human (vastus lateralis)				Mouse (EDL)	Rat (infraspinus)
	Male		Female		Male	Male
	Type 1	Type 2a	Type 1	Type 2a	(not typed)	(not typed)
CSA (μm^2)	4880 - 6900	5270 - 8380	3870 - 5470	4010 - 5610	1850 - 3080	5290 - 8010
F_o (mN)	0.79 - 1.17	1.02 - 1.54	0.64 - 0.97	0.71 - 1.07	0.14 - 0.25	0.55 - 0.97
sF_o (kPa)	142 - 182	165 - 210	156 - 193	172 - 214	67 - 94	102 - 131
n	129	160	149	207	37	94

Table 3. Typical characteristics of healthy, adult fibers from human vastus lateralis¹⁰, mouse extensor digitorum longus¹ and rat infraspinus² muscles. Optimal sarcomere lengths were set at 2.7 μm for human fibers^{7,8} and 2.5 μm for both mouse (36,37) and rat fibers (38). Experimental L_f ranges (25th and 75th quartiles) were 1.39-1.73 mm, 1.17-1.53 mm and 1.32-1.59 mm for human, mouse and rat respectively. Ranges shown indicate the 25th and 75th quartiles and n is the number of fibers tested.

The most common problems experienced during testing include a suture loop slip, which results in a force response with a “catch” such as that illustrated in **Figure 10A**, and a partial or full thickness tear of the fiber, which results in a force response that returns abruptly toward or to (break) zero while the fiber is still immersed in activating solution (**Figure 10B**). If a slip, tear or break occurs during an experiment, the fiber should be discarded and the data excluded, though maintaining a record of fiber failures can also be informative¹¹. Another negative outcome that may be encountered is the premature activation of the fiber while in the pre-activating solution (**Figure 10C**). Partial activation in the pre-activating solution suggests significant cross-well contamination (i.e., an unintentional increase in calcium concentration in the pre-activating well). In this instance, all baths should be aspirated and rinsed well with deionized water. Drying the dividing surfaces between the chambers is also recommended as moisture or condensation in these areas may lead to wicking of solution between baths. The decision to include or exclude data will ultimately depend on the experimental focus and should thus be considered when designing the study.



250 μ m

Figure 1: Suture loop (10-0 monofilament nylon suture).

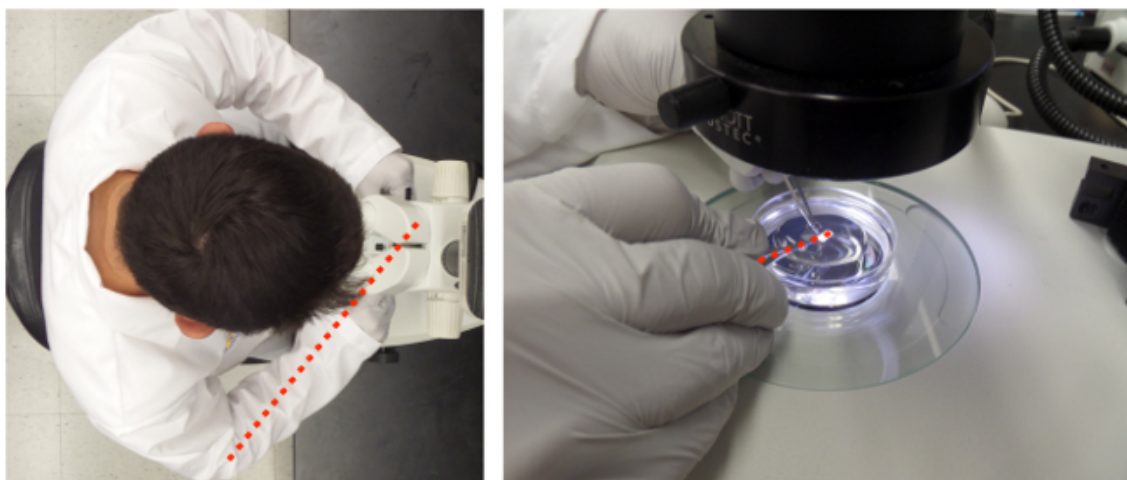


Figure 2: Bundle dissection. Forceps are in left hand, microdissection scissors are in right hand. Red line indicates the favorable orientation of the wrist and scissors with the longitudinal axes of the fibers.

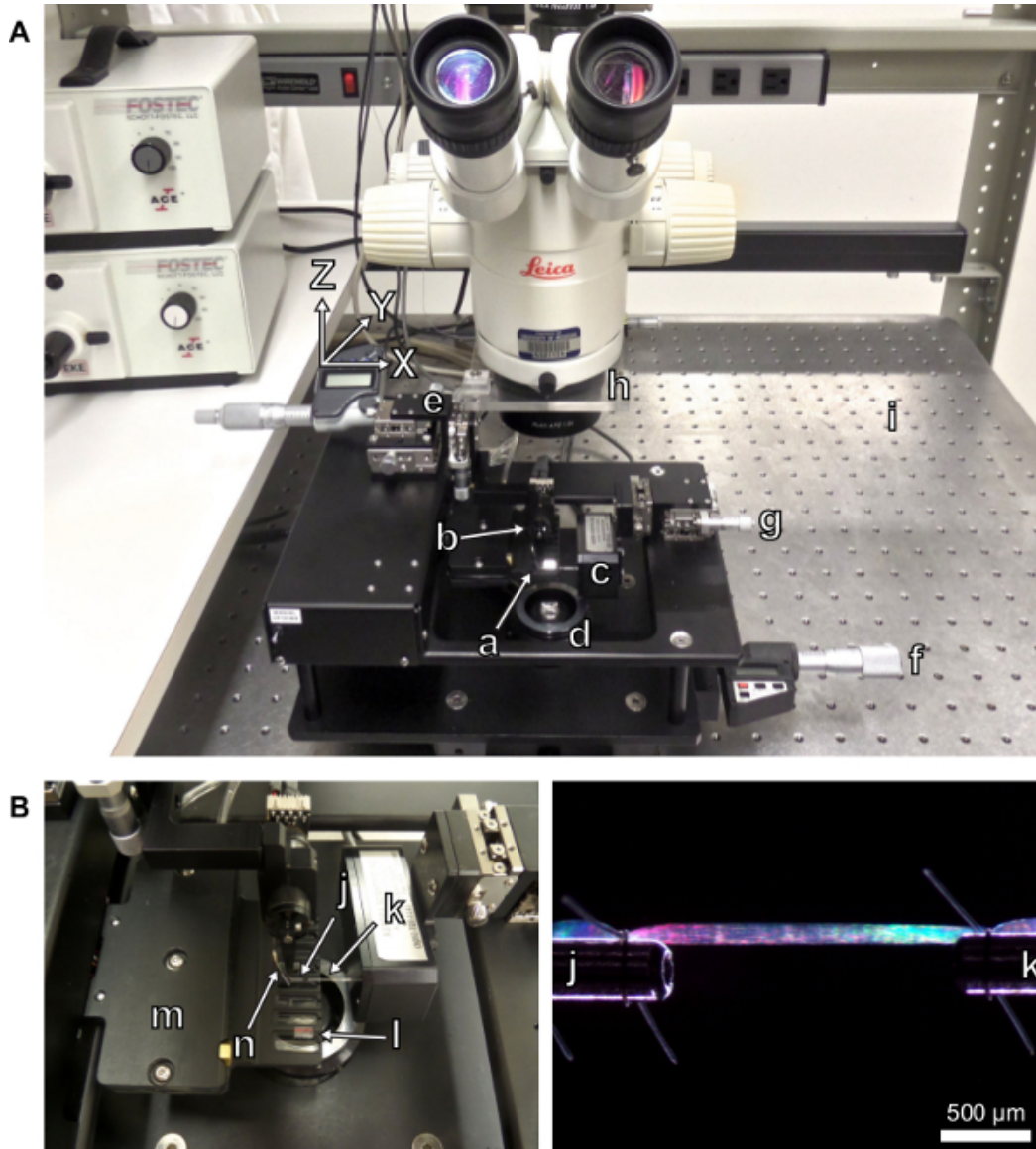


Figure 3: (A) Testing apparatus with labeled components. (a) Experimental chambers with transparent bottoms. (b) Length-controller. (c) Force-transducer. (d) Light source. (e) Length-controller x-y-z micrometer drive with digital display. (f) Stage micrometer drive with digital display. (g) Force-transducer x-y-z micrometer drive. (h) Platform for calibrated laser-diffraction target screen. (i) Vibration isolation table. (B) Close-up view of the experimental chambers. (j) Stainless steel attachment surface extending from the length-controller. (k) Stainless steel attachment surface extending from the force-transducer. (l) Side-view prism. (m) Housing for thermoelectric cooling modules. (n) Thermocouple for reporting chamber temperature.

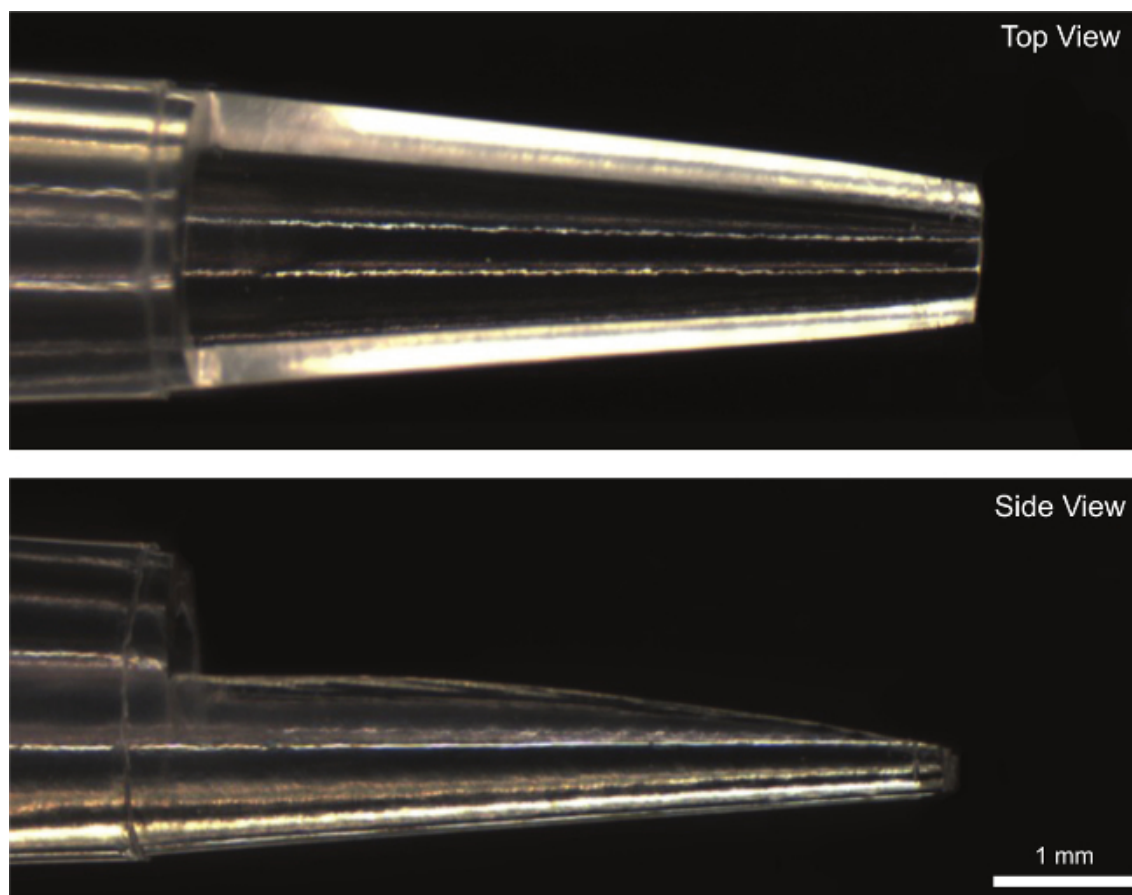


Figure 4: Modified 100 μ l pipet tip used to transfer fiber from dissection dish to experimental chamber.

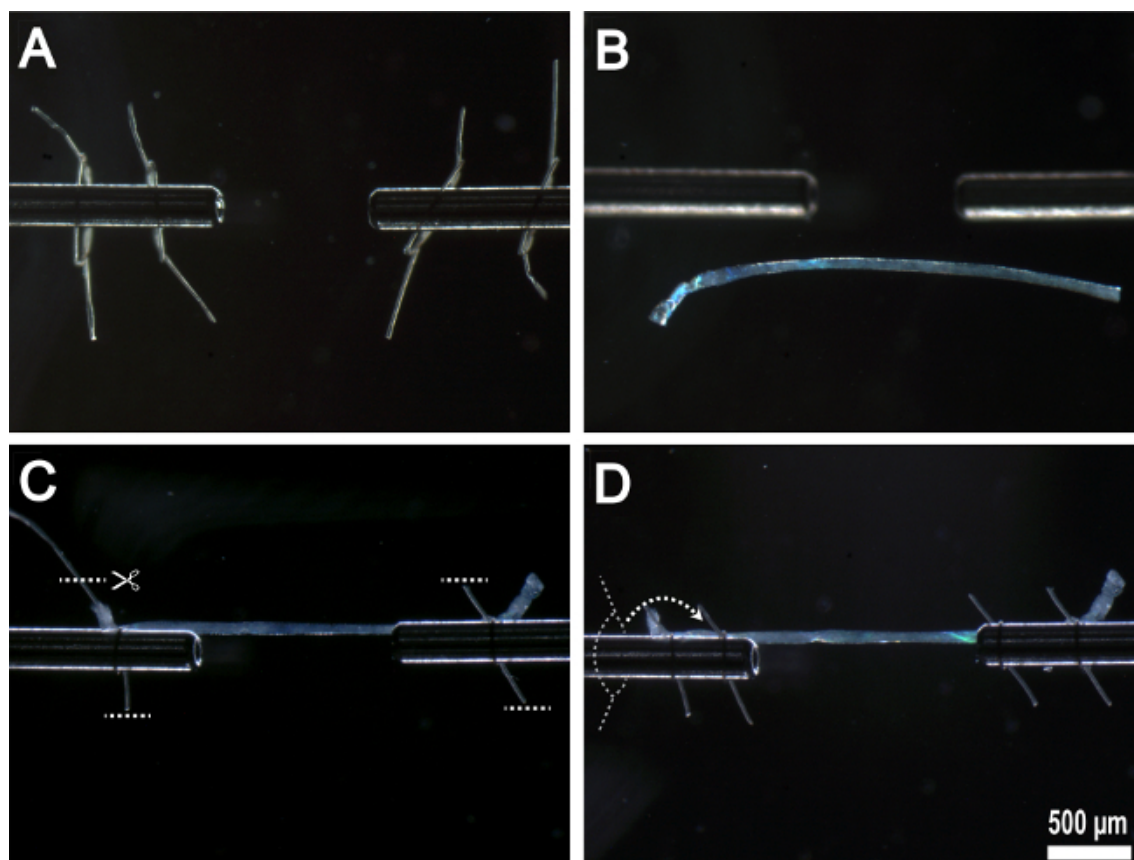


Figure 5: Mounting single fiber onto experimental apparatus. (A) Prepared suture loops threaded onto stainless steel attachment surfaces. (B) Fiber transferred to experimental chamber. (C) Fiber anchored to stainless steel attachment surfaces by first pair of suture loops with excess suture removed. (D) Second pair of suture loops threaded over the top of first suture loops and tied in place.

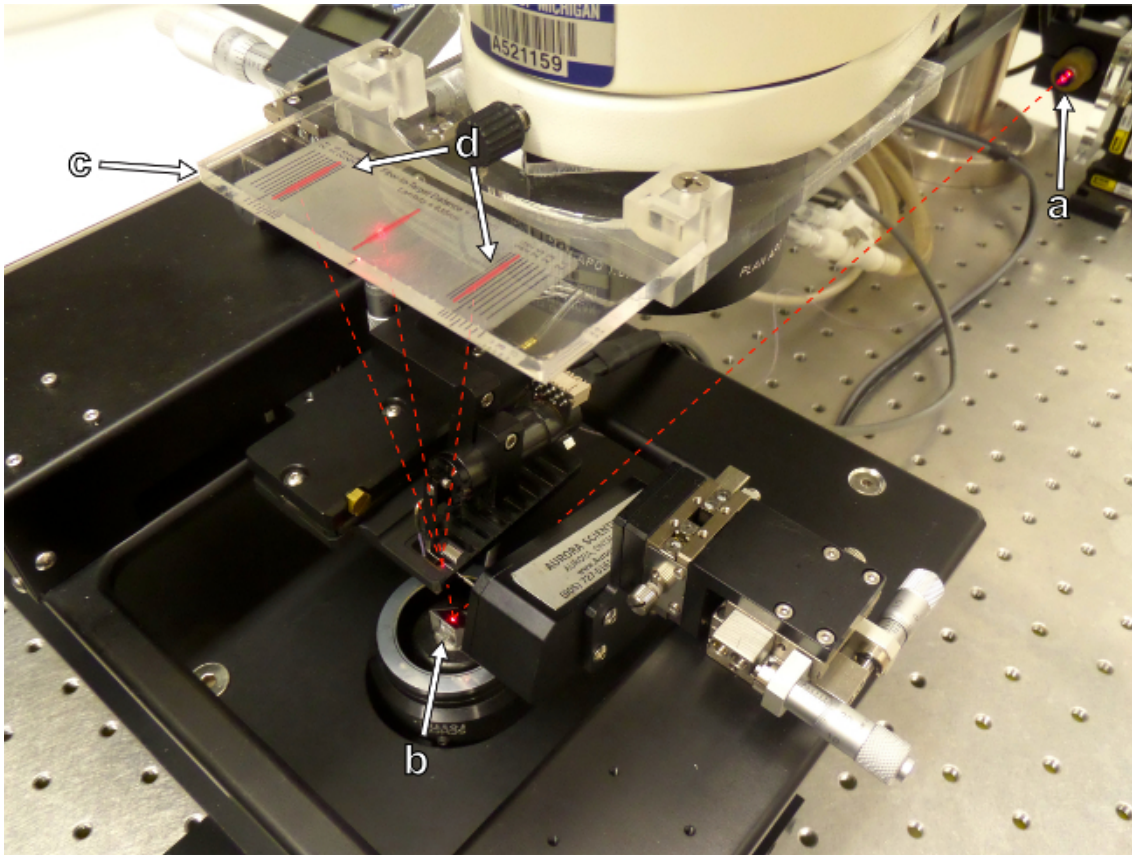
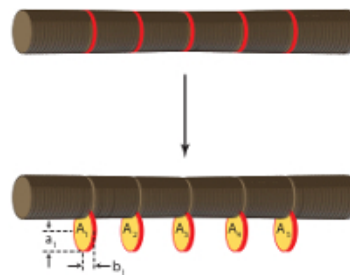
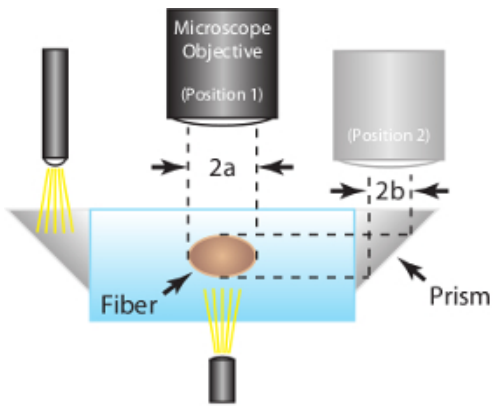


Figure 6: Sarcomere length is assessed by the projection of a laser interference pattern onto a calibrated target screen. (a) Laser source. (b) Mirror. (c) Target screen. (d) Laser interference pattern.



$$CSA = \frac{\sum_{i=1}^5 A_i}{5} = \frac{\sum_{i=1}^5 \pi a_i b_i}{5}$$

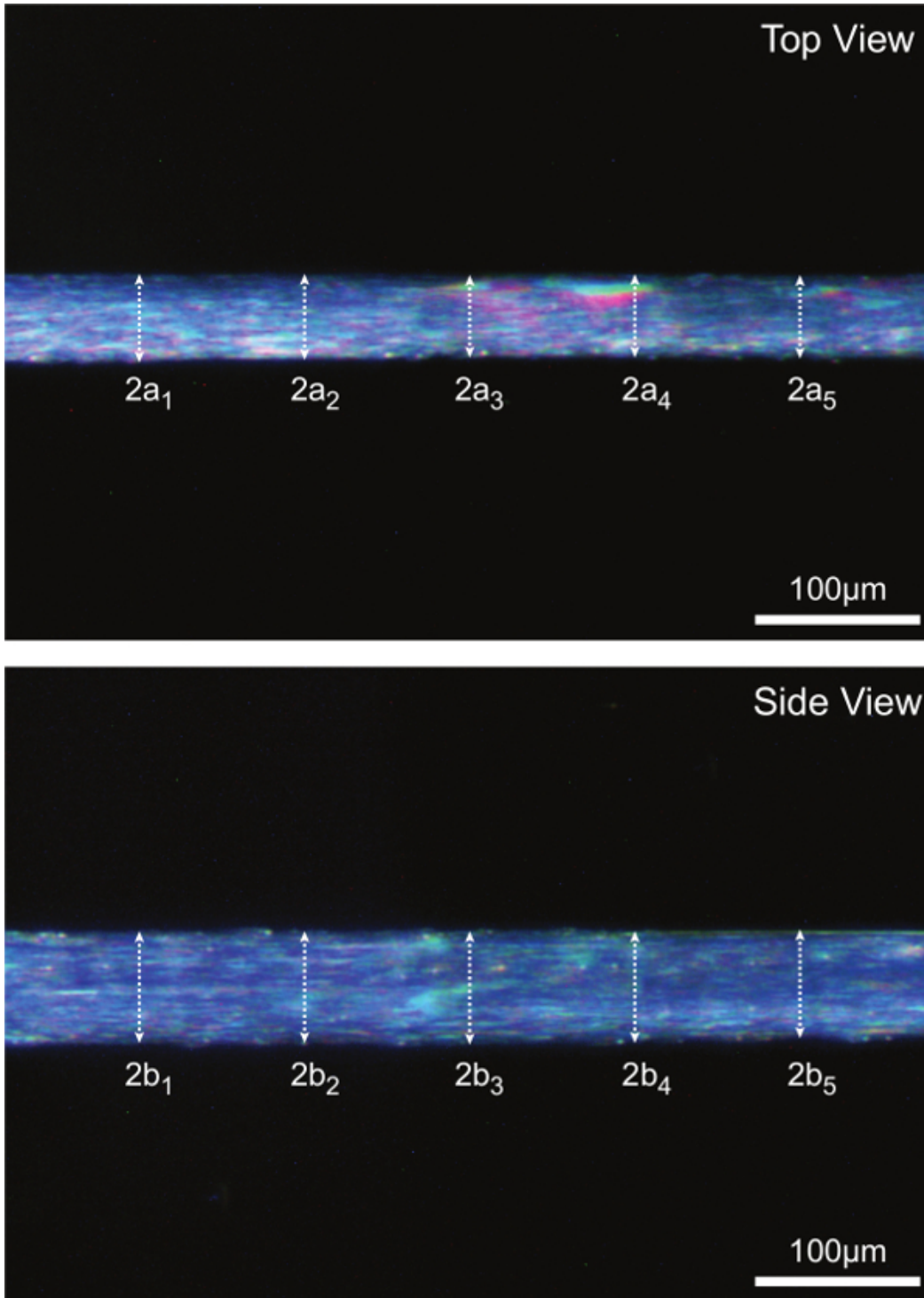
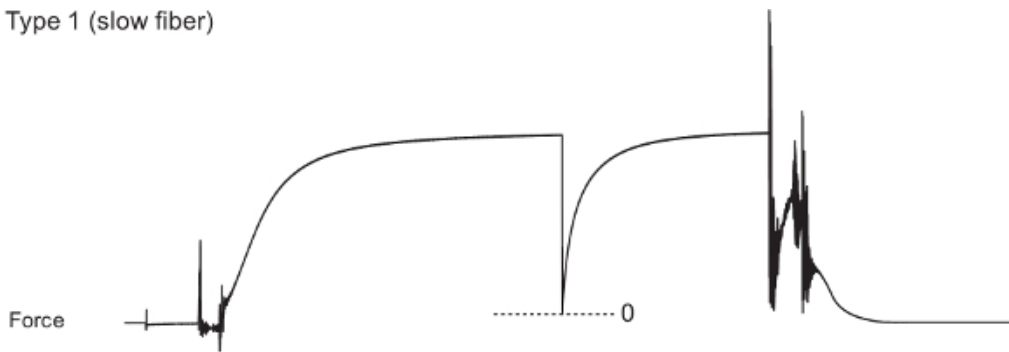


Figure 7: (A) Determination of fiber cross-sectional area at optimal sarcomere length (human = 2.7 μm). Assuming an elliptical cross-section, CSA is calculated for each of five locations along the fiber midsection and the mean of the five individual measurements is reported as fiber CSA. 2a represents top view diameter and is one axis of the ellipse, 2b represents side view diameter and is the other axis of the ellipse. (B) Representative fiber images illustrating each of the five corresponding diameter measurements taken in both the top and side view.

A. Type 1 (slow fiber)



B. Type 2a (fast fiber)

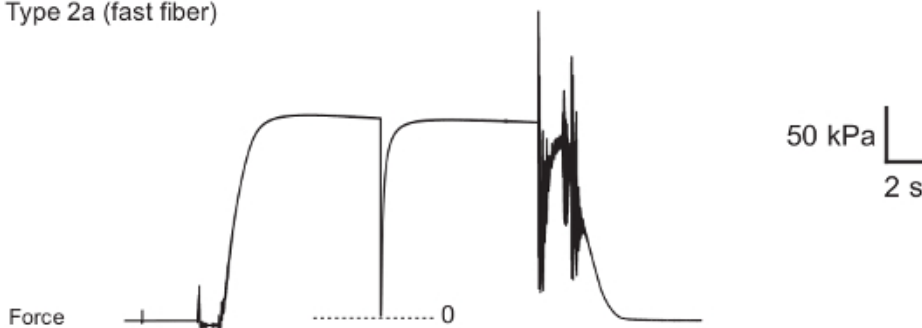


Figure 8: Representative force traces from healthy human *vastus lateralis* muscle fibers. (A) Type 1 fiber (CSA: 5710 μm^2 , F_o : 0.89 mN and sF_o : 156 kPa). (B) Type 2a fiber (CSA: 9510 μm^2 , F_o : 1.66 mN and sF_o : 174 kPa). Fiber myosin heavy chain type was determined through the use of electrophoretic separation and silver-staining techniques²².

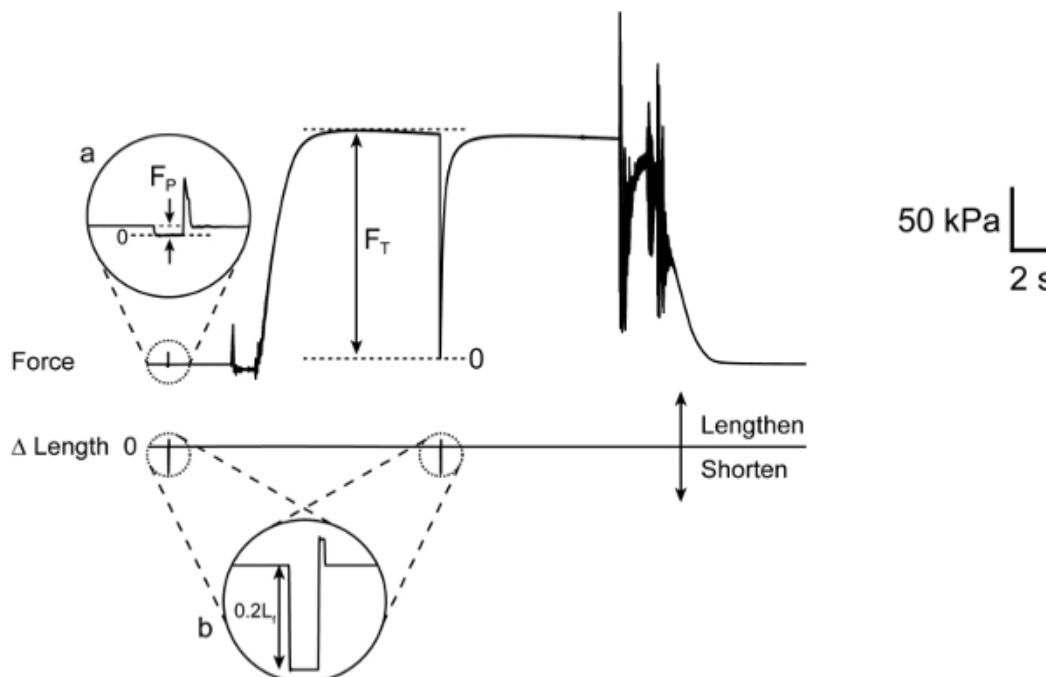


Figure 9: Calculation of maximum active force (F_o). (a) Expanded view of fiber force response during slack-inducing movement of length-controller initiated in pre-activating solution. F_p is the force required to maintain a sarcomere length of 2.7 μm with the fiber at rest. (b) Expanded view of length-controller slack-inducing movement. Note that $F_o = F_T - F_p$.

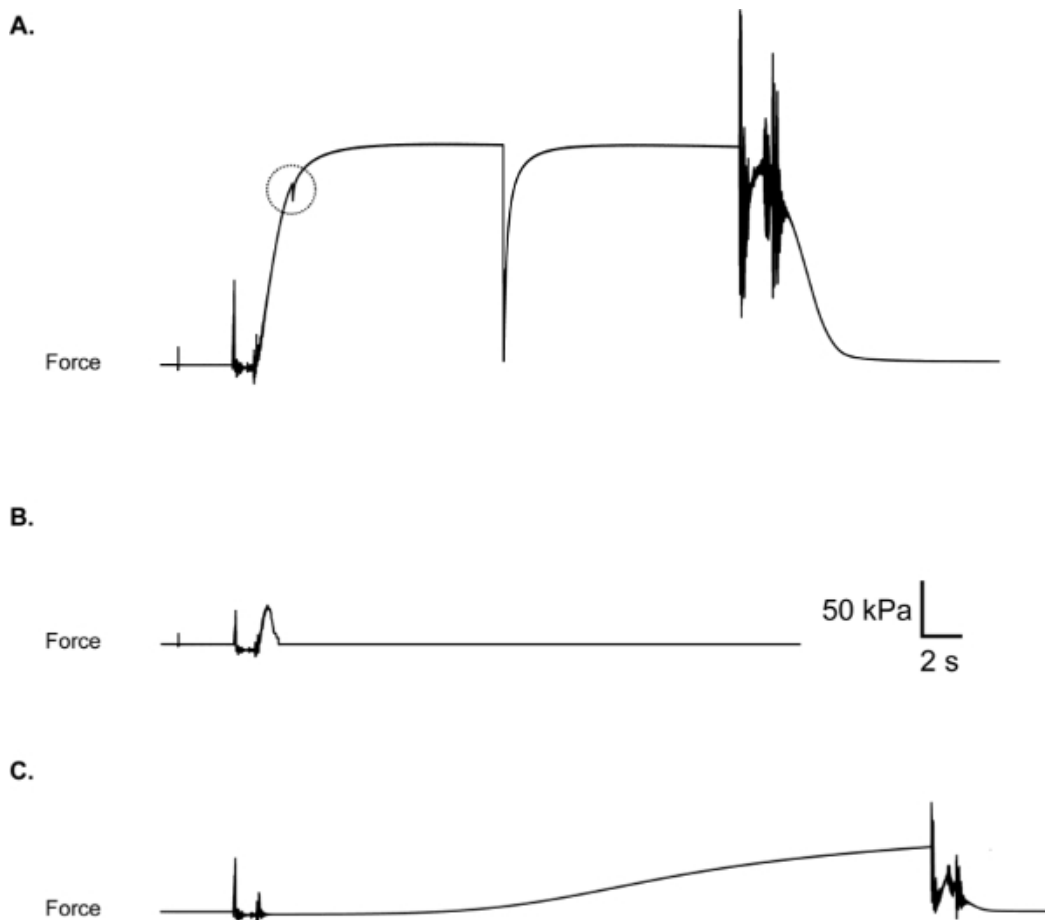


Figure 10: (A) Suture loop slip, evidenced by a “catch” in force trace during the rise of force. Check to be sure loops are secure before activating the fiber. (B) Fiber break during activation. May be due to poor fiber integrity or aggressive fiber treatment during suture loop placement. (C) Premature partial fiber activation due to contamination of pre-activation chamber with Ca^{2+} .

Discussion

Assessments of the contractile properties of permeabilized single skeletal muscle fibers are used to investigate muscle function in a wide variety of contexts. Examples include studies that have evaluated the effects of aging¹², exercise^{10,13,14}, spaceflight¹⁵, injury^{2,3,16}, drug treatments^{17,18}, disease¹⁹ and genetic manipulation^{20,21} on fiber structure and function. Due to the ability to directly assess the contractile performance of myofibrils in their native configuration, this technique provides an attractive platform from which to form an understanding of myofibrillar function absent of potentially confounding effects that are present when neuromuscular signal transmission and excitation-induced calcium release are included in the system under study. Furthermore, functional testing of single fibers can be used to complement contractile protein identification results such as those obtained through immunohistochemistry or gel electrophoresis + western blot²².

One of the primary functions of skeletal muscle is to generate force. Consequently sF_o , a measure of the intrinsic force generating capability of a contractile system, is of great interest to muscle physiologists. Reliable estimates of sF_o require accurate measures of both fiber CSA and F_o . Since fibers are, in general, neither circular in cross-section, nor uniform in CSA along their length, great care should be taken when estimating CSA. To this end, measurements are made at several locations along the length of the fiber and, at each location, from two perspectives separated by 90°. Reliable measures of F_o require attention to several details including accounting for passive force, adjusting sarcomere length to maximize overlap of thick and thin filaments, employing an activating solution with a calcium concentration that results in maximal activation, maintaining the desired experimental temperature, and maintaining optimal storage conditions (temperature and duration) of the fibers prior the day of the experiment.

While the steps outlined here describe the procedure for evaluating maximum isometric force, it is frequently desirable to evaluate other important functional qualities of skeletal muscle fibers. This can be achieved by extending the experimental protocol to include additional mechanical manipulations of the fiber. For example, measurement of the speed at which the fiber shortens against a series of different loads allows determination of the force-velocity relationship, from which force-power and velocity-power relationships can be computed^{10,23,24}. Additionally, the speed of unloaded shortening can be determined by employing the “slack test”²⁵, which consist of applying a series of slack-inducing shortening steps and measuring the time required by the fiber to remove the slack. Another kinetic parameter that is frequently reported is k_r , the rate constant for force redevelopment following a mechanical perturbation that temporarily detaches all crossbridges²⁶. Finally, the relationship between calcium concentration and active force generation (the “force-pCa relationship”) is often of interest¹⁸ and can be determined

by exposing the fiber to a series of solutions with calcium concentrations ranging from below the threshold for activating the contractile system to those sufficient to elicit maximum activation and therefore maximum force (F_0).

Though much of the mentioned equipment is needed for assessing single fiber contractility, other equipment is not absolutely necessary. The length-controller, for example, is essential for any experimental protocol that requires rapid or precise lengthening or shortening of the fiber, but is not absolutely necessary for evaluating maximum isometric force (though a zero-force level in the force record must still be identified by some means). The prisms that allow observation of the fiber from the side, while useful for assessing cross-sectional area, are not absolutely necessary when positioning the fiber within the experimental chamber. Furthermore, alternative means for exposing the fiber to the various experimental solutions could be employed, including devising a manually-operated system of chambers or a single chamber that allows for rapid filling and emptying of solutions. Finally, while sub-physiological experimental temperatures such as 15 °C are commonly used to improve the reproducibility of mechanical measurements^{1,2,3,5,8,12,17,27}, it is possible to generate valid data at other temperatures^{23,28} as long as the effects of temperature on solution properties (calcium concentration, pH, etc.) are taken into consideration.

The compositions of the testing solutions are among the most critical aspects of the permeabilized fiber techniques described here. Considerations regarding solution composition are complex and beyond the scope of this article. The solutions described in Step 5 of the protocol section are designed with an emphasis on rapid activation of the permeabilized fiber upon its transfer from pre-activating to activating solutions while maintaining a constant ionic strength, cationic composition, and osmolarity^{6,29}. Other approaches to solution composition have been employed with notable success by other research groups and typically make use of published binding constants and computational tools^{27,30,31}. The concentrations of calcium ions in the various activating solutions is particularly important in studies involving submaximal activation such as force-pCa evaluations. For experiments in which fibers are fully activated, such as those described here, the calcium concentration in the activating solution typically exceeds by a comfortable margin that required to achieve maximum force, making its precise knowledge less critical. Addition of creatine phosphate is important for buffering the intramyofibrillar ATP and ADP fluctuations that would otherwise be associated with contractile activity. Creatine kinase is required to catalyze the phosphate transfer from creatine phosphate to ADP. Under experimental conditions that result in high ATP turnover rates, including working at high temperatures or measuring high-speed shortening in fast fibers³², creatine kinase must be added to the solution to supplement the endogenous creatine kinase that remains bound to the fiber. For less demanding experimental conditions, the ATP regeneration system is less critical²⁷.

Limitations of the permeabilized single fiber technique include the following. The data generated by these tests define the contractile properties of the specific myofibrillar unit that was attached to the experimental apparatus. Consequently, this captures only a small fraction of the entire multinucleated fiber from which the segment was obtained which, in turn, represents a small fraction of the total number of fibers within the muscle. Investigators should thus consider carefully the sampling required to support any conclusions drawn from the experiments. Additionally, evaluating the impact of an exercise training intervention on fiber function presumes that the fibers evaluated were indeed recruited during the training. Though the protocol attempts to mimic the natural intracellular milieu of the fiber, the sarcolemma permeabilization process is non-specific and necessarily allows soluble intracellular constituents to freely diffuse into the bathing solutions. A further consequence of the membrane permeability is a change in the osmotic balance evidenced by a swelling in fiber volume³³. The fiber swelling increases the distance between actin and myosin filaments resulting in reduced calcium sensitivity of the myofilament system^{34,35}, but can be reversed by the introduction of large, osmotically active compounds³⁴. A final limitation to consider is the consequence of the technique used to attach fibers to the experimental apparatus. This invariably requires distorting the spatial relationship within the filament system at and near the attachment points, with attending functional deficits. Specifically, the regions of the fiber at and adjacent to the attachment points are functionally compromised and thereby contribute artifactual series elasticity to the measurement system.

In summary, we have described a means by which to assess the force-generating capacity of chemically permeabilized skeletal muscle fibers *in vitro*. Though the focus of this article has been on the assessment of maximum isometric force generating capacity of human skeletal muscle fibers, the experimental approach can be modified and extended to determine a variety of kinetic parameters and relationships across a range of species, mammalian or otherwise.

Disclosures

Production and free access to this article is sponsored by Aurora Scientific

Acknowledgements

This work was supported by the following funding sources: R01-AR063649, AG-020591, F31-AR035931.

References

1. Mendias, C. L., Kayupov, E., Bradley, J. R., Brooks, S. V., Claflin, D.R. Decreased specific force and power production of muscle fibers from myostatin-deficient mice are associated with a suppression of protein degradation. *J Appl Physiol.* **111** (1), 185-91, doi:10.1152/jappphysiol.00126.2011, (2011).
2. Gumucio, J. P., Davis, M. E., Bradley, J. R., Stafford, P. L., Schiffman, C. J., Lynch, E. B., Claflin, D. R., Bedi, A., Mendias, C. L. Rotator cuff tear reduces muscle fiber specific force production and induces macrophage accumulation and autophagy. *J Orthop Res.* **30** (12), 1963-70, doi:10.002/jor.22168, (2012).
3. Mendias, C. L., Roche, S. M., Harning, J. A., Davis, M. E., Lynch, E. B., Sibilsky Enselman, E. R., Jacobson, J. A., Claflin, D. R., Calve, S., Bedi, A. Reduced muscle fiber force production and disrupted myofibril architecture in patients with chronic rotator cuff tears. *J Shoulder Elbow Surg.* **1** (4), 111-9. doi: 10.1016/j.jse.2014.06.037 (2015).
4. Moss, R. L. Sarcomere length-tension relations of frog skinned muscle fibres during calcium activation at short lengths. *J Physiol.* **292**, 177-192, (1979).

5. Chase, P. B., Kushmerick, M. J. Effects of pH on contraction of rabbit fast and slow skeletal muscle fibers. *Biophys J.* **53**, 935-946, doi:10.1016/S0006-3495(88)83174-6, (1988).
6. Moiescu, D. G., Thieleczek, R.. Calcium and strontium concentration changes within skinned muscle preparations following a change in the external bathing solution. *J Physiol.* **275**, 241-262, doi: 10.1113/jphysiol.1978.sp012188 (1978).
7. Walker, S. M., Schrodt, G.R. I Segment lengths and thin filament periods in skeletal muscle fibers of the Rhesus monkey and the human. *Anat Rec.* **178**, 63-81, doi:10.1002/ar.1091780107(1974).
8. Gollapudi, S.K., Lin, D. C. Experimental determination of sarcomere force-length relationship in type-1 human skeletal muscle fibers. *J Biomech.* **42**, 2011-2016, doi:10.1016/j.jbiomech.2009.06.013, (2009).
9. Brenner, B. Technique for stabilizing the striation pattern in maximally calcium-activated skinned rabbit psoas fibers. *Biophys J.* **41** (1), 99-102, doi:10.1016/S0006-3495(83)84411-7, (1983).
10. Clafflin, D. R., et al. Effects of high and low-velocity resistance training on the contractile properties of skeletal muscle fibers from young and older humans. *J Appl Physiol.* **111**, 1021-1030, doi:10.1152/jappphysiol.01119.2010, (2011).
11. Lynch, G. S., Faulkner, J. A., and Brooks, S. V. Force deficits and breakage rates after single lengthening contractions of single fast fibers from unconditioned and conditioned muscles of young and old rats. *Am J Physiol Cell Physiol.* **295**, C249-256. doi: 10.1152/ajpcell.90640, (2008).
12. Frontera, W. R., Rodriguez Zayas, A., Rodriguez, N. Aging of human muscle: understanding sarcopenia at the single muscle cell level. *Phys Med Rehabil Clin N Am.* **23**, 201-207, doi:10.1016/j.pmr.2011.11.012, (2012).
13. Malisoux, L., Francaux, M., Theisen, D. What do single-fiber studies tell us about exercise training? *Med Sci Sports Exerc.* **39** (7), 1051-1060, doi: 10.1249/mss.0b13e318057aeb, (2007).
14. Widrick, J. L., Stelzer, J.E., Shoepe, T.C., Garner, D.P. Functional properties of human muscle fibers after short-term resistance exercise training. *Am J Physiol Regulatory Integrative Comp Physiol.* **238**, 408-416, doi:10.1152/ajpregu.00120.2002, (2002).
15. Trappe, S. Effects of spaceflight, simulated spaceflight and countermeasures on single muscle fiber physiology. *J Gravit Physiol.* **9** (1), 323-326, (2002).
16. Malisoux, L., Jamart, C., Delplace, K., Nielens, H., Francaux, M., Thiesen, D. Effect of long-term muscle paralysis on human single fiber mechanics. *J Appl Physiol.* **102**, 340-449 doi:10.1152/jappphysiol.00609.2006, (2006).
17. Krivickas, L. S., Walsh, R., Amato, A. Single muscle fiber contractile properties in adults with muscular dystrophy treated with MYO-029. *Muscle Nerve.* **39**, 3-9, doi:10.1002/mus.21200, (2009).
18. Russell, A. J., et al. Activation of fast skeletal muscle troponin as a potential therapeutic approach for treating neuromuscular diseases. *Nature Medicine.* **18** (3), 352-356, doi:10.1038/nm.2618, (2012).
19. Krivickas, L. S., Yang, J. I., Kim, S. K., Frontera, W. R. Skeletal muscle fiber function and rate of disease progression in amyotrophic lateral sclerosis. *Muscle Nerve.* **26**, 636-643, doi:10.1002/mus.10257, (2002).
20. Mendias, C. L., Marcin, J.E., Calderon, D.R., Faulkner, J.A. Contractile properties of EDL and soleus muscles of myostatin-deficient mice. *J Appl Physiol.* **101**, 898-905, doi:10.1152/jappphysiol.00126, (2006).
21. Lynch, G.S., Rafael, J.A., Chamberlain, J.S., Faulkner, J.A. Contraction-induced injury to single permeabilized muscle fibers from mdx, transgenic mdx and control mice. *Am J Physiol Cell Physiol.* **279**, 1290-1294, (2000).
22. Mizunoya, Q., Wakamatsu, J., Tatsumi, R., Ikeuchi, Y. Protocol for high-resolution separation of rodent myosin heavy chain isoforms in a mini-gel electrophoresis system. *Anal Biochem.* **377**, 111-113, doi:10.1016/j.ab.2008.02.021, (2008).
23. Hill, A. V. The heat of shortening and the dynamic constants of muscle. *Proc R Soc Lond B Biol Sci.* **126**, 136-195, (1938).
24. Bottinelli, R., Canepari, M., Pellegrino, M.A., Reggiani, C. Force-velocity properties of human skeletal muscle fibres: myosin heavy chain isoform and temperature dependence. *J Physiol.* **495**, 573-586, doi:10.1113/jphysiol.1996.sp021617 (1996).
25. Edman, K.A. The velocity of unloaded shortening and its relation to sarcomere length and isometric force in vertebrate muscle fibres. *J Physiol.* **291**, 143-159, doi:10.1113/jphysiol.1979.sp012804 (1979).
26. Brenner, B., Eisenberg, E. Rate of force generation in muscle: Correlation with actomyosin ATPase activity in solution. *PNAS.* **83**, 3542-3546, (1986).
27. Moss, R. L. The effect of calcium on the maximum velocity of shortening in skinned skeletal muscle fibres of the rabbit. *J. Muscle Res. Cell Motil.* **3**, 295-311, doi:10.1007/BF00713039 (1982).
28. Pate, E., Wilson, G.J., Bhimani, M., Cooke, R. Temperature dependence of the inhibitory effects of orthovanadate on shortening velocity in fast skeletal muscle. *Biophys J.* **66**, 1554-1562. Doi:10.1016/S0006-3495(94)80947-6 (1994).
29. Ashley, C. C., Moiescu, D. G. Effect of changing the composition of the bathing solutions upon the isometric tension-pCa relationship in bundles of crustacean myofibrils. *J Physiol.* **270**, 627-652, doi:10.1113/jphysiol.1977.sp011972 (1977).
30. Godt, R. E. Calcium-activated tension of skinned muscle fibers of the frog. Dependence on magnesium adenosine triphosphate concentration. *J Gen Physiol.* **63**, 722-739, doi: 10.1085/jgp.63.6.722 (1974).
31. Fabiato, A., Fabiato, F. Calculator programs for computing the composition of the solutions containing multiple metals and ligands used for experiments in skinned skeletal muscle cells. *Journal de Physiologie (Paris).* **75**, 463-505, (1979).
32. Chase, P. B., Kushmerick, M.J. Effect of physiological ADP concentrations on contraction of single skinned fibers from rabbit fast and slow muscles. *Am J Physiol.* **268**, C480-489, doi:10.1016/S0006-3495(98)77855-5 (1995).
33. Godt, R.E., Maughan, D.W. Swelling of skinned muscle fibers of the frog. *Biophysical Journal.* **19**, 103-116, doi:10.1016/S0006-3495(77)85573-2 (1977).
34. Kawai, M., Wray, J. S., Zhao, Y. The effect of lattice spacing change on cross-bridge kinetics in chemically skinned rabbit psoas muscle fibers. *Biophys J.* **64**, 187-196, doi:10.1016/S0006-3495(93)81356-0 (1993).
35. Millman, B.M. The filament lattice of striated muscle. *Physiol Rev.* **78** (2), 359-391, (1998).
36. Edman, K. A. Contractile properties of mouse single muscle fibers, a comparison with amphibian muscle fibers. *J Exp Biol.* **208**, 1905-1913, doi:10.1113/jphysiol.2001.016220 (2005).
37. Phillips, S. K, and Wolejda, R.C. A comparison of isometric force, maximum power and isometric heat rate as a function of sarcomere length in mouse skeletal muscle. *Pflügers Archiv.* **420**, 578-583. doi: 10.1007/Bf00374636 (1992).
38. Stephenson, D.G., Williams, D.A. Effects of sarcomere length on the force-pCa relation in fast and slow-twitch skinned muscle fibres from the rat. *J Physiol.* **333**, 637-653, doi:10.1113/jphysiol.1982.sp014473 (1982).